Dynamical simulation of the optical response of photosynthetic pigments†

M. Belén Oviedo, Christian F. A. Negre and Cristián G. Sánchez*

Received 10th December 2009, Accepted 11th March 2010
First published as an Advance Article on the web 27th April 2010
DOI: 10.1039/b926051j

From time integration of the electron dynamics under a density functional tight binding Hamiltonian in the presence of external time varying electric fields, we obtain the absorption spectra of a series of chlorophylls and bacteriochlorophylls. We obtain good agreement with the observed experimental energies as well as with fully *ab initio* results in the literature for the main absorption bands. As a first step towards an atomistic description of energy transfer between chromophores in photosynthetic antenna systems we calculate the coupling energy between the excitations of two chlorophyll *a* molecules as a function of the distance as well as the transfer of energy between these when one of them is subjected to laser illumination.

Introduction

Photosynthesis represents the main source of energy for Earth's biosphere. Its primary process, the excitation of photosynthetic pigments and posterior driving of electron transfer at the reaction center, occurs with a very large quantum yield.[1] Understanding this unusual efficiency poses a remarkable challenge given the size of the multiprotein complexes involved and the fact that the process is, in essence, quantum dynamical and therefore must be treated as such. Recent experimental evidence suggests that the high quantum yield of photosynthesis might rely on suppression of environmental decoherence of excitons within antenna complexes.[2,3] Coherent exciton evolution would allow parallel exploration of a multitude of relaxation pathways increasing efficiency relative to classical hopping dynamics.[2] Needless to say, complete understanding of the molecular mechanisms of photosynthesis would provide an invaluable tool for the engineering of self-assembling nano-devices capable of harvesting sunlight in a cheap and efficient manner.

Given the multiscale nature of the problem at hand, a variety of theoretical approaches have been applied to its study, ranging from the successful Gouterman model[4] that can explain the main bands of the absorption spectra of chlorophylls to *ab initio* prediction of chromophore spectra[5–7] and studies of the quantum dynamics of excitation transfer between pigments.[8] Time dependent density functional theory has recently become a *de facto* standard for the study of optical response of molecular systems[9] and has proved successful for the description of the excitations of chlorophylls[6,7,10] despite its well known limitation of underestimating the energy of charge transfer excitations.[11,12]

Hamiltonians capable of describing the dynamics of excitation transfer between chromophores coupled to their environment[13] provide description of the coherent evolution of excitons. These models require information on the excitation energies of individual pigments embedded in their proteic environment, as well as inter-chromophore couplings, parameters which are normally extracted from fitting of appropriate Hamiltonians to a variety of experimental data.[14]

Chlorophylls and bacteriochlorophylls represent a core component of photosynthetic organisms. Without them, light cannot be absorbed and therefore they represent the first fundamental step towards energy storage in photosynthetic organisms.[1] Fig. 1 shows a generic chlorophyll molecule, where the structure of the porphyrin ring, the numbering of carbon atoms and the polarization axes of the most important excitations are depicted. By convention, the y molecular axis of chlorophylls and bacterioclorophylls is defined as the axis passing through the N atoms of rings A and C, conversely the x molecular axis is the one passing through the N atoms of rings B and D. The z axis is taken to be perpendicular to the plane of the molecule.[1] If the molecule is illuminated with light polarized along the y molecular axis it stimulates an electronic transition at long wavelength called the Q_y transition. On the other hand, there is a transition of weaker intensity when the molecule is illuminated with light polarized along the x axis, this transition is called Q_x. Soret bands appearing at shorter wavelengths possess mixed polarization.[1]

Ideally, in order to advance towards a theoretical understanding of the primary process of photosynthesis, one would like an atomistic model, capable of describing the photophysics of individual photosynthetic pigments as well as the dynamical evolution of their coupled excitations when embedded within a proteic environment. The work we show here represents a first step towards this goal. By studying the full dynamical evolution of the one electron density matrix within a DFTB (Density Functional Tight Binding) Hamiltonian[15,16] in response to different kinds of external time-dependent electric fields, both optical absorption and energy transfer within chromophore arrangements can be studied. We show results for the optical absorption spectra of a series of chlorophylls and bacterio-chlorophylls and compare these to both experimental and *ab initio* results in the literature as well as the coupling between

Departamento de Matemática y Física, Facultad de Ciencias Químicas, INFIQC, Universidad Nacional de Córdoba, Ciudad Universitaria, Córdoba, X5000HUA, Argentina.
E-mail: cgsanchez@fcq.unc.edu.ar

† Electronic supplementary information (ESI) available: Optimized structure coordinates for all chromophores. See DOI: 10.1039/b926051j

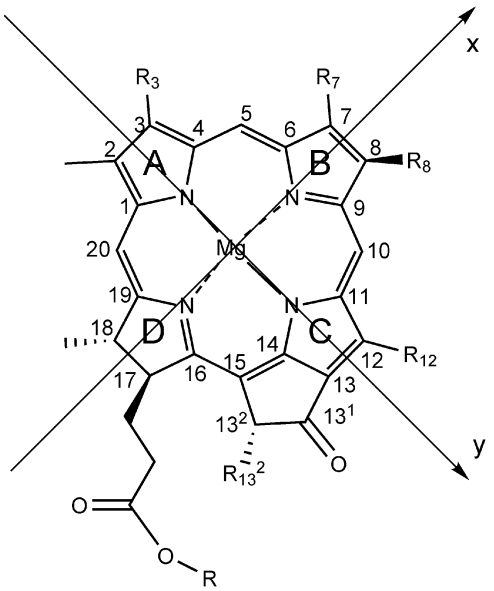

Fig. 1 Generic molecular model of chlorophyll showing the structure of the porphirinic ring, the numbering of carbon atoms within it and the direction of polarization of its most important excitations. For the calculations described in the text the R substituent (a phytyl chain in most cases) has been replaced by a hydrogen atom.

excitations of a chlorophyll dimer at a series of intermolecular distances. We expect our work to serve as a validation of the time dependent DFTB method as applied to the study of photosynthetic pigments and their interactions.

Computational method

The self consistent density functional tight-binding method (SCC-DFTB) is a very efficient scheme to describe the electronic structure of large molecular systems.[16] It is based on the second order expansion of the Kohn–Sham energy functional around a reference density of neutral atomic species. The DFTB+ code[17] is a sparse matrix based implementation of the DFTB method. We have used this code as obtained from the authors for all geometry optimizations as well as calculations of the Hamiltonian and overlap matrix elements and the initial single electron density matrix. Several different incarnations of time-dependent SCC-DFTB have been described in the literature, both within the restriction of linear response[18,19] and implementing the full non-linear dynamics.[20] Our implementation differs from that of reference[20] in that it propagates the one electron density matrix instead of the single particle orbitals.

The SCC-DFTB hamiltonian is an intermediate step between a simple tight-binding Hamiltonian and a fully *ab initio* density-functional theory (DFT) representation of the electronic structure. The Hamiltonian matrix elements are obtained as follows:[16]

$$H_{\mu\nu} = \langle \phi_\mu | \hat{H}^0 | \phi_\nu \rangle + \frac{1}{2} S_{\mu\nu} \sum_k^N (\gamma_{ik} + \gamma_{jk}) \Delta q_k \qquad (1)$$

where orbitals μ and ν belong to atoms i and j, respectively. Here, $\Delta q_k = q_k - q_k^0$ is the difference between the charge of the isolated atom q_k^0 and the charge q_k obtained by Mulliken population analysis when atom k is conforming the molecule. The function of inter-atomic separation $\gamma_{ij} = \gamma_{ij}(U_i, U_j, |\vec{R}_i - \vec{R}_j|)$, interpolates smoothly between onsite interactions with a strength $U_i = \gamma_{ii}$ and the bare Coulomb interaction at large separation. The latter parameter is related to the chemical hardness of the atomic species. Here, $S_{\mu\nu} = \langle \phi_\mu | \phi_\nu \rangle$ are the overlap matrix elements and $H^0_{\mu\nu}$ are the matrix elements of the non SCC-TB hamiltonian within the Slater-Koster parametrization. $H^0_{\mu\nu}$ and $S_{\mu\nu}$ are calculated from first principles for a minimal Slater orbital basis and tabulated for all pairs of species. For the calculations shown here we have used the "mio-0-1" parameter set[16] for elements O, N, C and H as well as the corresponding parameters for magnesium containing molecules described in ref. 21. The DFTB method has been extensively validated for the prediction of molecular structures and reaction energies.[22] The prediction of optical properties is outside the scope for which the method had been initially proposed, and has only very recently been applied to this area. In this respect the method inherits both the successes (and failures) of time dependent density functional theory, but at a much lower computational cost.[23]

Mulliken charges q_i are obtained by summing over every orbital contribution as follows:

$$q_i = \frac{1}{2} \sum_K^{occ} n_K \sum_{\mu \in i} \sum_\nu^N (c^*_{\mu K} c_{\nu K} S_{\mu\nu} + c^*_{\nu K} c_{\mu K} S_{\nu\mu}) \qquad (2)$$

where n_K are the molecular orbital fillings and $c_{\mu K}$ are the expansion coefficients of ψ_{GS} obtained by solving the eigenvalue problem in the atomic orbital basis. In matrix notation we have:

$$q_i = \frac{1}{2} \sum_{\mu \in i} (\rho S + S\rho)_{\mu\mu} \qquad (3)$$

where $\rho_{\mu\nu} = \sum_K^{occ} c^*_{\mu K} n_K c_{K\nu}$ is the one electron density matrix.

We first perform a molecular structure optimization† followed by a determination of the self-consistent DFTB Hamiltonian and the one electron density matrix for the system ground state (GS). This task is carried out by using the DFTB+ code as provided by the authors. We then introduce an initial perturbation in the shape of a Dirac delta pulse ($\hat{H} = \hat{H}^0 + E_0 \delta(t - t_0)\hat{\mu}$) to the initial GS density matrix previously obtained.[24] After the pulse application, the density matrix evolves in time and its evolution can be calculated by time integration of the Liouville–von Newmann equation of motion in the non-orthogonal basis:

$$\frac{\partial \hat{\rho}}{\partial t} = \frac{1}{i\hbar} (S^{-1} \hat{H}[\hat{\rho}] \hat{\rho} - \hat{\rho} \hat{H}[\hat{\rho}] S^{-1}) \qquad (4)$$

This model may be viewed as an intermediate step between full time-dependent density-functional theory (TDDFT) in the adiabatic local-density approximation (ALDA)[25] and simpler time-dependent tight-binding (TDTB) implementations.[26] Note that $\hat{H}$ depends on $\hat{\rho}$ through the onsite charges introducing non linear effects in the dynamics, renormalizing the excitations of the non self-consistent DFTB Hamiltonian.[20] In the linear response regime, when the applied electric field pulse is small, the response is linear and the dipole moment is:

$$\mu(t) = \int_{-\infty}^{\infty} \alpha(t - \tau) E(\tau)\, d\tau \qquad (5)$$

where $\alpha\ (t - \tau)$ is the polarizability along the axis over which the external field $E(t)$ is applied. The absorption spectrum is proportional to the imaginary part of the frequency dependent polarizability, obtained from the Fourier transform of the time dependent dipole moment, after deconvolution of the applied electric field ($E(t) = E_0\delta(t_0 - t)$ with $E_0 = 0.01$ V/Å):

$$\alpha(\omega) = \frac{\mu(\omega)}{E_0} \qquad (6)$$

In order to make the dipole signal die out within the simulated time window an exponential damping with a time constant of 10 fs is applied before transforming to frequency space, uniformly broadening all of the spectral lines.

This method determines the frequency dependent polarizability along the direction of the initially applied field. The average of the polarizability along the three cartesian axes is taken as the absorption spectra of the system. We have checked that spectra are independent of the magnitude of the applied initial electric field indicating that the simulations are done within the linear response regime under which the frequency dependent polarizability can be extracted from the response using eqn (6).

Results and discussion

The optical absorption spectra of chlorophylls and bacteriochlrophylls are well characterized and have been studied in detail since their discovery in the early 19th century. Spectra present essentially two characteristic absorption bands. The first one, called Soret, can be found in the UV region and is a complex band composed of a large series of electronic transitions. The second, called Q is in the visible region of the spectrum. It is known from the simple model proposed by Gouterman in 1961 that Q and Soret bands are generated by $\pi \rightarrow \pi^*$ excitations stimulated by light polarized in the direction of the molecular plane. The typical absorption regions of these bands, in particular the lack of absorption within the green area of the spectrum, are responsible for the characteristic color of most photosynthetic organisms.

Fig. 2 shows a comparison between optical absorption spectra calculated using the methods described in the previous section and the corresponding experimental data[27] for a series of photosynthetic pigments. A very good correlation can be observed between the predicted and observed absorption bands. Calculated results reproduce the main differences between the spectra, with the exception of the relative intensity of the Q and Soret bands in some cases.

In the spectrum of chlorophyll *a* (Fig. 2a) a single Q band is observed called Q_y band. In Fig. 3 we show the different spectra obtained when the molecule is excited by a polarized light over the main molecular axes. The solid line spectrum corresponds to the polarization over the y axis while the dashed line spectrum corresponds to the x axis polarization. It can be seen that the band that appears at the longest wavelengths corresponds to the Q_y transition (solid line) while the band which appears with lower intensity (dashed line) corresponds to the Q_x band which appears around 600 nm, these band is obscured by the Q_y band in the total spectrum (Fig. 2a).

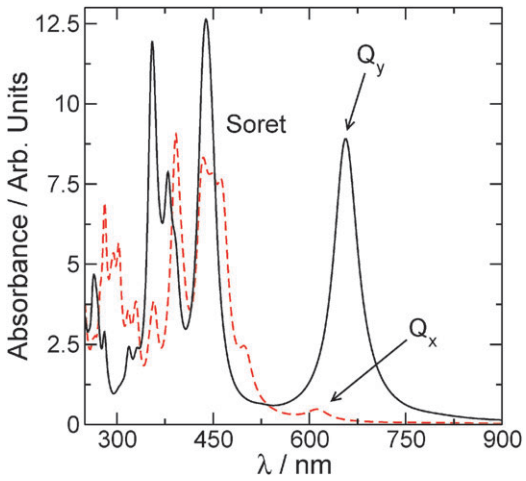

Fig. 3 Absorption spectra of chlorophyll *a* for light polarized along the x (dashed line) and y (full line) molecular axes.

Chlorophyll *b* (Fig. 2b) differs from chlorophyll *a* (Fig. 2a) on the substituent present at C_7, where the methyl group of chlorophyll *a* has been replaced by a formyl group in the former. This change has the effect of displacing the Q_y band some 10 nm into the UV region and a similar shift of the Soret band to lower energies. This is attributed to the effect the C═O double bond has on the conjugated system.[28] This effect is qualitatively reproduced by the calculated spectra.

The basic difference between bacteriochlorophylls and chlorophylls lays in the structure of the pyrrole rings. In the case of bacteriochlorophylls both B and D rings are reduced, whereas in the case of chlorophylls only the ring D is reduced. Comparing the spectra of bacteriochlorophylls (Fig. 2c and d) and chlorophylls (Fig. 2a and b) it can be observed that Q_y bands move to longer wavelengths and their intensity is increased respect to those in chlorophylls, also, the Q_x band is more intense and can be clearly identified and Soret bands do not show much change. Bacteriochlorophyll *b* has an ethydene group at C_8 extending the π conjugated system and further lowering the absorption energy of the bands. The theoretical and experimental spectra for bacteriochlorophyll *e* are shown on Fig. 2e. The spectra are similar to those of chlorophyll's since the porphyrin ring is only partially reduced. All of these trends are qualitatively reproduced by the theoretical results.

In order to evaluate quantitatively the accuracy of the time dependent DFTB method for the prediction of the absorption energies of the spectral bands more relevant to the description of light harvesting photophysics we have compared in Fig. 4 the difference between the experimental and predicted band positions for our results as well as those obtained from TDDFT by Burda and collaborators.[28] In the case of the Q_x band (Fig. 4a), the absolute error of the predictions of time dependent DFTB is smaller than 20 nm in all cases, whereas the TDDFT results show errors between 40 and 80 nm. In the case of Q_y bands (Fig. 4b), our results show errors of less than 60 nm whereas TDDFT shows errors between 70 and 100 nm. Not much information exists in the literature[9] that can allow us to evaluate the prediction of relative intensities, based on the results of Baroni *et al.*

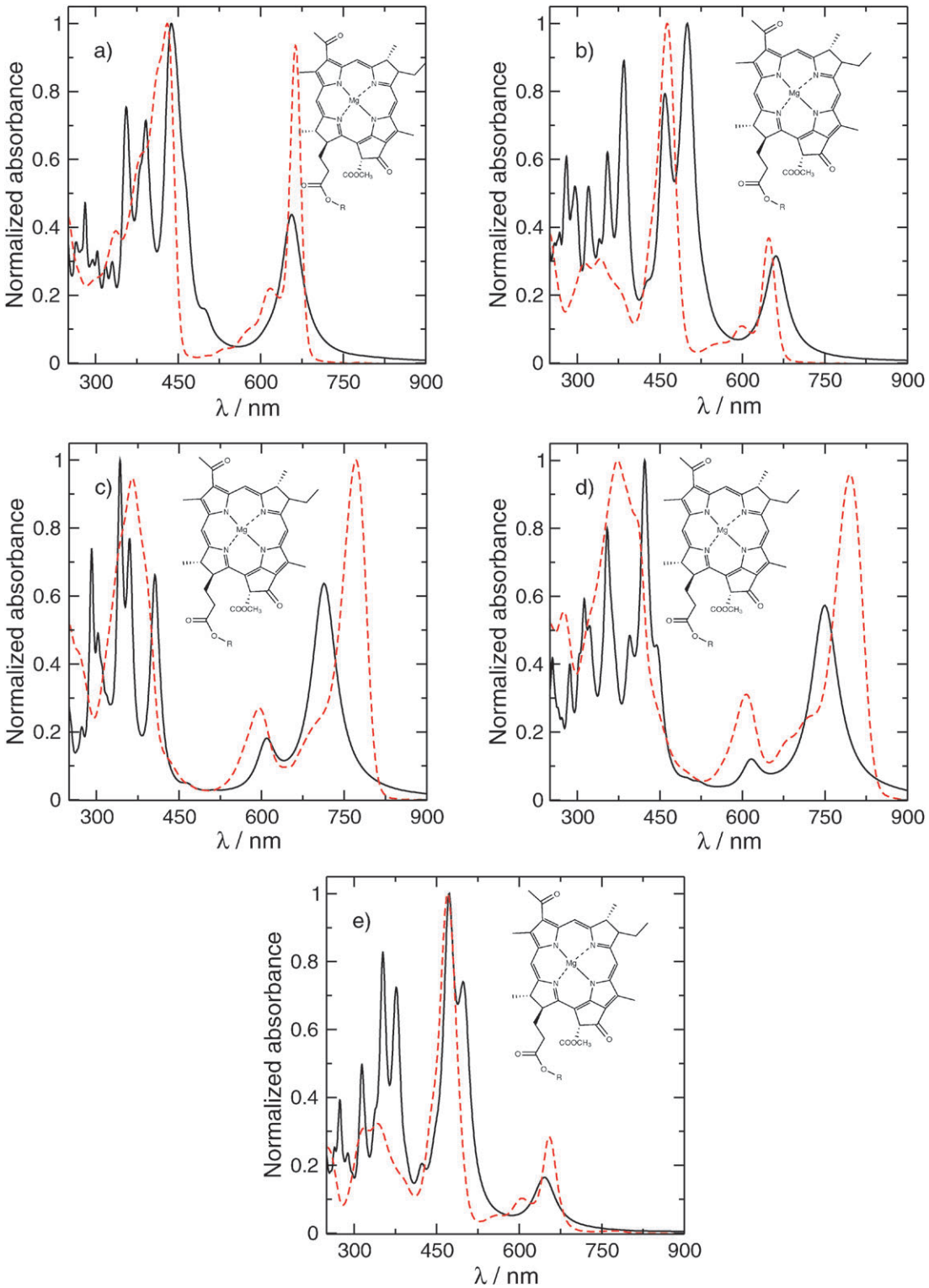

Fig. 2 Comparison between calculated and experimental optical absorption spectra for a series of chlorophylls and bacteriochlorophylls: (a) chlorophyll *a*, (b) chlorophyll *b*, (c) bacteriochlorophyll *a*, (d) bacteriochlorophyll *b*, (e) bacteriochlorophyll *e*. Full lines correspond to the theoretical results obtained as explained in the text, dashed lines show experimental results from ref. 27.

(based on Fig. 7 of ref. 10) despite having lower success with the prediction of energies, the prediction of the relative intensities of *Q* and Soret bands by TDDFT seems to be more accurate, at least for chlorophyll *a*.

As a first step towards description of excitation coupling and energy transfer between pigments, we have studied the absorption spectra and response to laser illumination of a chlorophyll *a* dimer aligned along the *y* axis (with monomers

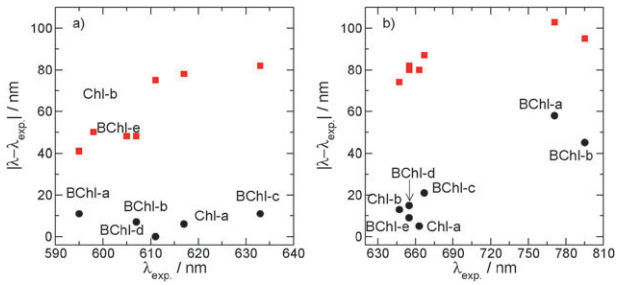

Fig. 4 Comparison of relative errors in the prediction of absorption energy of the Q_x (a) and Q_y (b) bands of chlorophylls and bacteriochlorophylls by the methods described in the text (circles) and *ab initio* TDDFT results (squares) in the literature.[28]

at their isolated equilibrium geometries). In the case of a chromophore dimer, coupling between the excitations breaks the degeneracy between them. The dimer has two excitations separated by twice the value of the coupling energy between monomer excitations. The lower energy one is the symmetric linear combination of the monomer excitations and is the only active one of the two since the monomer dipoles oscillate in phase. Fig. 5 shows the energy difference between the lowest absorption energy band (Q_y) of the dimer (ω) as a function of the distance between Mg atoms, d, and the energy of the same excitation in the monomer ω_0. Following the reasoning just exposed, this difference is equal to the coupling energy between monomer excitations which is maximal for the chose orientation. The solid line in Fig. 5 is a power-law fit of the results which results in the following equation

$$|\omega - \omega_0| = 62.8\ d^{-3.20} \qquad (7)$$

As can be concluded from the plot, the results start to deviate from the expected power law behaviour whenever the distance between magnesium atoms is lower than 30 Å, this difference being most evident at distances lower than about 17 Å when the calculated points move above the power law fit. The fitted exponent of 3.20 is over the value of 3 that would be expected from a purely dipolar interaction indicating that for the range of distances covered by the calculated results (which is lower than approximately four molecular diameters) higher order terms that the purely dipolar are important in the interaction.

From a time dependent perspective, coupling between excitations residing at different chromophores is the cause of excitation energy transfer between them. Fig. 6 shows the variation of the dipole moment of two chlorophyll *a* molecules aligned along the y axis, separated by 22.0 Å in response to laser illumination tuned to the monomer excitation. The external field is applied only to one of the monomers, the dipole moment of which is plotted in the upper panel of Fig. 6. As can be expected for an applied field within the linear response regime and in the absence of any dissipative mechanism the molecular dipole moment oscillation amplitude grows linearly with time. The second molecule dipole moment (plotted in the lower panel of Fig. 6) grows quadratically as expected, being excited by the linearly growing dipole of the first molecule. After about 150 fs of constant illumination the second molecule has reached about a fifth of the excitation of the first.

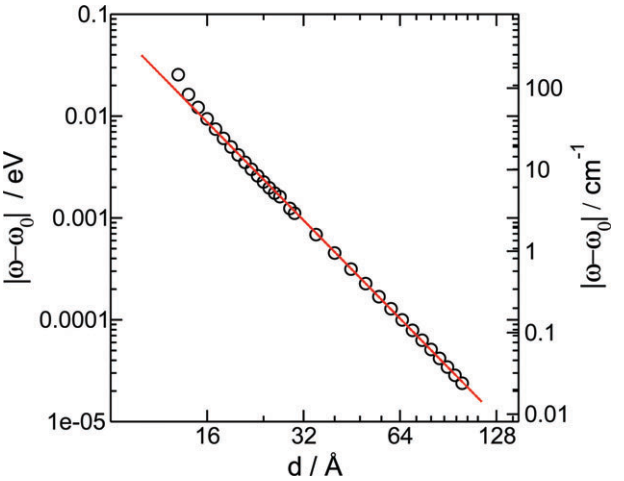

Fig. 5 Log–log plot of the difference between the Q_y excitation energy of a chlorophyll *a* molecule (ω_0) and its dimer (ω) as a function of the distance between corresponding magnesium atoms, the solid line corresponds to a power law fit of the data. Molecules are aligned along the y axis direction.

Conclusions

In this paper we have presented a method to propagate the equation of motion of the one electron density matrix within the DFTB framework under the influence of external time dependent electric fields. This method allows to analyze linear response properties such as absorption spectra as well as fully time dependent phenomena outside the linear regime. As a starting point we have calculated the absorption spectra of chlorophylls and bacterioclorophylls obtaining excellent agreement with experimental results, given the approximate nature of the method. The method can quantitatively predict the energies of Q_x and Q_y bands of photosynthetic pigments with similar or higher accuracy than TDDFT calculations, with the advantage that it can deal with very large systems.

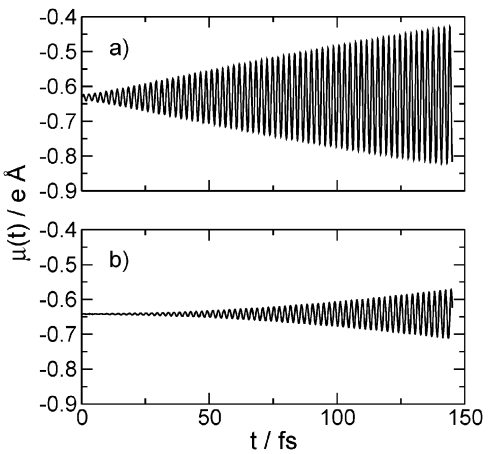

Fig. 6 Time dependent variation of the dipole moment of individual component molecules of a chlorophyll *a* dimer in response to laser illumination. The external field is applied only to one of the molecules (a) while the other (b) is stimulated by the oscillating field of the first. The distance between Mg atoms is 22.0 Å and the molecules are aligned along the y axis.

We have also shown the dependence of the coupling energy between excitations for a chlorophyll *a* dimer as well as how the method can describe excitation transfer between chromophores in real time. The simulation technique we have applied could, in principle, allow for the estimation of solvent effects on the spectra by including explicitly the first solvation shell in the simulation and appropriately sampling the solvent configurational space. Vibronic coupling is an important issue that has been left out of the work at its present stage and could be dealt with from a dynamical perspective by including the quantum dynamics of the relevant vibrational coordinates in the simulation by a formalism such as correlated electron–ion dynamics.[29,30]

Acknowledgements

We acknowledge support by Consejo Nacional de Investigaciones Científicas y Técnicas (CONICET) through grant PIP 112-200801-000983 and ANPCYT through grant Program BID 1728/OC-AR PICT No 629. M.B.O. and C.F.A.N. are grateful for studentships from CONICET. We thank Prof. Marcus Elstner for the provision of DFTB+ Slater-Koster tables for magnesium containing molecules from ref. 21.

References

1 R. E. Blankenship, *Molecular Mechanisms of Photosynthesis*, Blackwell Publishing Limited, Oxford, 2002.
2 G. S. Engel, T. R. Calhoun, E. L. Read, T.-K. Ahn, T. Mančal, Y.-C. Cheng, R. E. Blankenship and G. R. Fleming, *Nature*, 2007, **446**, 782–786.
3 H. Lee, Y.-C. Cheng and G. R. Fleming, *Science*, 2007, **316**, 1462–1465.
4 M. Gouterman, *J. Mol. Spectrosc.*, 1961, **6**, 138–163.
5 J. Linnanto and J. Korppi-Tommola, *Phys. Chem. Chem. Phys.*, 2006, **8**, 663–687.
6 D. Sundholm, *Chem. Phys. Lett.*, 1999, **302**, 480–484.
7 D. Sundholm, *Phys. Chem. Chem. Phys.*, 2003, **5**, 4265–4271.
8 Y.-C. C. Cheng and G. R. Fleming, *Annu. Rev. Phys. Chem.*, 2009, **60**, 241–262.
9 F. Buda, *Photosynth. Res.*, 2009, **102**, 437–441.
10 D. Rocca, R. Gebauer, Y. Saad and S. Baroni, *J. Chem. Phys.*, 2008, **128**, 154105.
11 M. G. Dahlbom and J. R. Reimers, *Mol. Phys.*, 2005, **103**, 1057–1065.
12 A. Dreuw and M. Head-Gordon, *J. Am. Chem. Soc.*, 2004, **126**, 4007–4016.
13 A. Ishizaki and G. R. Fleming, *Proc. Natl. Acad. Sci. U. S. A.*, 2009, **106**, 17255–17260.
14 J. Adolphs and T. Renger, *Biophys. J.*, 2006, **91**, 2778–2797.
15 D. Porezag, T. Frauenheim, T. Köhler, G. Seifert and R. Kaschner, *Phys. Rev. B: Condens. Matter*, 1995, **51**, 12947–12957.
16 M. Elstner, D. Porezag, G. Jungnickel, J. Elsner, M. Haugk, Th. S. Suhai and G. Seifert, *Phys. Rev. B: Condens. Matter Mater. Phys.*, 1998, **58**, 7260–7268.
17 B. Aradi, B. Hourahine and T. Frauenheim, *J. Phys. Chem. A*, 2007, **111**, 5678–5684.
18 T. A. Niehaus, S. Suhai, F. D. Sala, P. Lugli, M. Elstner, G. Seifert and T. Frauenheim, *Phys. Rev. B: Condens. Matter Mater. Phys.*, 2001, **63**, 085108.
19 F. Wang, C. Y. Yam, G. Chen, X. Wang, K. Fan, T. A. Niehaus and T. Frauenheim, *Phys. Rev. B: Condens. Matter Mater. Phys.*, 2007, **76**, 045114.
20 T. A. Niehaus, D. Heringer, B. Torralva and T. Frauenheim, *European physical journal D: Atomic, Molecular and Optical Physics*, 2005, **35**, 467–477.
21 Z.-L. Cai, P. Lopez, J. R. Reimers, Q. Cui and M. Elstner, *J. Phys. Chem. A*, 2007, **111**, 5743–5750.
22 T. Krüger, M. Elstner, P. Schiffels and T. Frauenheim, *J. Chem. Phys.*, 2005, **122**, 114110.
23 T. Niehaus, S. Suhai, F. Della Sala, P. Lugli, M. Elstner, G. Seifert and T. Frauenheim, *Phys. Rev. B: Condens. Matter Mater. Phys.*, 2001, **63**, 085108.
24 K. Yabana and G. F. Bertsch, *Phys. Rev. B: Condens. Matter*, 1996, **54**, 4484–4487.
25 E. Runge and E. K. U. Gross, *Phys. Rev. Lett.*, 1984, **52**, 997.
26 C. F. A. Negre and C. G. Sánchez, *J. Chem. Phys.*, 2008, **129**, 034710.
27 N.-U. Frigaard, K. L. Larsen and R. P. Cox, *FEMS Microbiol. Ecol.*, 1996, **20**, 69–77.
28 Z. Vokácová and J. V. Burda, *J. Phys. Chem. A*, 2007, **111**, 5864–5878.
29 A. P. Horsfield, D. R. Bowler, A. J. Fisher, T. N. Todorov and C. G. Sánchez, *J. Phys.: Condens. Matter*, 2004, **16**, 8251–8266.
30 A. P. Horsfield, D. R. Bowler, A. J. Fisher, T. N. Todorov and C. G. Sánchez, *J. Phys.: Condens. Matter*, 2005, **17**, 4793–4812.